



# Consequences of replacing EGFR juxtamembrane domain with an unstructured sequence

Lijuan He & Kalina Hristova

Department of Materials Science and Engineering, Johns Hopkins University, Baltimore, MD 21218.

SUBJECT AREAS:  
BIOPHYSICAL CHEMISTRY  
MEMBRANE PROTEINS  
MEMBRANE BIOPHYSICS  
PROTEINS

Received  
21 August 2012

Accepted  
29 October 2012

Published  
14 November 2012

Correspondence and  
requests for materials  
should be addressed to  
K.H. (kh@jhu.edu)

**EGFR is the best studied receptor tyrosine kinase. Yet, a comprehensive mechanistic understanding of EGFR signaling is lacking, despite very active research in the field. In this paper, we investigate the role of the juxtamembrane (JM) domain in EGFR signaling by replacing it with a (GGS)<sub>10</sub> unstructured sequence. We probe the effect of this replacement on (i) EGFR phosphorylation, (ii) EGFR dimerization and (iii) ligand (EGF) binding. We show that the replacement of EGFR JM domain with a (GGS)<sub>10</sub> unstructured linker completely abolishes the phosphorylation of all tyrosine residues, without measurable effects on receptor dimerization or ligand binding. Our results suggest that the JM domain does not stabilize the inactive EGFR dimer in the absence of ligand, and is likely critical only for the last step of EGFR activation, the ligand-induced transition from the inactive to active dimer.**

**E**GF is a receptor tyrosine kinase (RTK) which plays a critical role in cell proliferation, differentiation, survival and migration<sup>1,2</sup>. It also plays a complex role in carcinogenesis and cancer progression, and is thus an attractive candidate for anticancer therapies<sup>1,3</sup>. While there are significant benefits of anti-EGFR agents in some solid tumors including colorectal, neck, lung, and pancreatic tumors, many challenges remain in the improvement of the targeted EGFR therapies<sup>4,5</sup>. In part, this is due to a lack of comprehensive mechanistic understanding of EGFR signaling, despite very active research in the field.

EGFR, like all RTKs, consists of a ligand-binding extracellular (EC) domain, a single transmembrane domain and an intracellular portion composed of a juxtamembrane (JM) sequence, a kinase domain related to soluble kinases, and a C-terminal tail. EGFR activation is initiated upon EGFR dimerization, which brings the two kinase domains in close proximity. Ligand binding to the dimer induces a conformational change which propagates into the intracellular domain, and as a result one of the kinase domains catalyzes the phosphorylation of critical tyrosine residues on the C-terminal tail of the neighboring receptor<sup>6</sup>. This is followed by the phosphorylation of additional intracellular tyrosine residues, which serve as binding sites for docking proteins. Upon recruitment and/or phosphorylation, these docking proteins initiate intracellular signaling cascades that control growth, differentiation, and motility<sup>7–9</sup>.

EGFR has been the most widely and in-depth studied RTK. Thus, we now have extensive knowledge about many of the specific interactions that are critical for EGFR signal transduction. For instance, it is well known that EGFR extracellular (EC) domains mediate tight dimer-stabilizing contacts in the presence of bound ligands<sup>10,11</sup>. The EGFR dimer is further stabilized by contacts between the two TM domains, which form sequence-specific dimers in the membrane<sup>12,13</sup>. The active EGFR kinase dimers are asymmetric, with the C-lobe of one kinase contacting the N-lobe of the second kinase; these contacts are critical for phosphate transfer and for kinase activation<sup>9</sup>.

Recently, evidence has emerged that the JM domain of EGFR, connecting the TM and the catalytic domains, is important for EGFR dimer stabilization and for EGFR signaling. In particular, the active EGFR dimer has been proposed to be stabilized by direct contacts between the two JM domains, as well as contacts between the JM domain and the neighboring kinase<sup>14</sup>. Furthermore, the deletion of EGFR JM domain has been shown to have multiple consequences such as altered EGFR dimerization<sup>14</sup>, aberrant ligand binding<sup>15</sup> and decreased phosphorylation<sup>16</sup>. A mechanistic model of how EGFR JM domain induces these effects and regulated EGFR signaling, however, is lacking.

In this paper, we revisit the role of the JM domain in EGFR signal transduction, by investigating the consequences of replacing it with a (GGS)<sub>10</sub> flexible linker. This experimental design is dictated by a concern that the deletion of the JM domain in some experiments could affect signaling by introducing structural constraints within



the EGFR dimer. For example, removal of the JM domain may bring the bulky catalytic domains too close to the intimately interacting  $\alpha$ -helical TM domains. As a result, the observed effects on EGFR activation will be due to steric hindrance and thus may not give insights into the role of the JM domain in wild-type EGFR signaling.

Here we probed the effect of the replacement on EGFR activation and on EGFR dimerization. We further performed ligand titration experiments to determine if the substitution affects ligand binding. We show that the replacement of EGFR JM domain with a (GGG)<sub>10</sub> linker completely abolishes the phosphorylation of all tyrosine residues. Unlike experiments in which the JM is deleted, however, the substitution has no effects on receptor dimerization or on ligand binding, over the ligand concentration range of 10 to 2500 ng/ml. Our results demonstrate that the JM domain does not stabilize the inactive EGFR dimer in the absence of ligand, and is likely critical only for the last step of EGFR activation, the ligand-induced transition from the inactive to active dimer.

## Results

**Replacement of EGFR JM domain by a (GGG)<sub>10</sub> flexible linker.** To investigate the role of the JM domains on EGFR function, we designed a chimeric receptor, EGFR-GGS, in which the JM domain is replaced by a (GGG)<sub>10</sub> sequence (Figure 1). The (GGG)<sub>X</sub> sequence has been demonstrated to lack a regular secondary structure and to be very flexible<sup>17</sup>. The plasmid was created as described in Materials and Methods. Briefly, the oligonucleotides encoding EGFR JM domain (EGFR amino acids 650–680) were removed by digestion, and annealed oligonucleotides encoding ten GGS repeats were inserted in their place.

**EGFR JM domain is required for EGFR phosphorylation.** CHO cells were transfected with either pcDNA3.1-EGFR or pcDNA3.1-EGFR-GGS, or the pcDNA 3.1(+) empty vector. 24 hours after transfection, cells were starved for another day, and then treated with the growth factor EGF. After lysis, the cell lysates were subjected to Western blotting. To investigate the effect of JM domain replacement on EGFR phosphorylation, we used two different anti-phospho-Tyr antibodies. The first of them, anti-P-Tyr1068, is specific for phosphorylated tyrosine 1068 in EGFR. The second one, 4G10, is a non-specific anti-phospho-Tyr

antibody that is reactive to all phospho-tyrosines. In Figure 2A, we see no anti-P-Tyr1068 and weak 4G10 antibody bands in the absence of ligand (lane 1: EGFR; lane 3: EGFR-GGS). Upon EGF addition, the intensities of the anti-P-Tyr1068 and the 4G10 antibody bands are increased for EGFR (lane 4), indicative of increased phosphorylation. For EGFR-GGS (lane 6), we see no anti-P-Tyr1068 staining and only a very weak 4G10 staining band which is also present in the control cells in the presence of ligand (and thus should not be attributed to EGF-GGS, lane 5). These results demonstrate that the substitution of the JM domain with the (GGG)<sub>10</sub> linker dramatically reduces EGFR's ability for cross-phosphorylation and activation. At the same time, the substitution does not affect receptor expression. Indeed, the expression levels of EGFR and EGFR-GGS, as probed by the anti-EGFR antibodies, are very similar (lanes 1 and 3, and 5 and 6). Thus, the substitution of the JM domain with an unstructured sequence abolished EGFR activation.

To ensure that receptor overexpression in the described transient transfection experiments is not distorting the results; we created cell lines that stably express the EGFR and EGFR-GGS receptors as described in Materials and Methods. Briefly, HEK 293 cells were transfected with the plasmids encoding EGFR and EGFR-GGS. Twenty four hours after transfection, the cell culture medium was replaced by selective medium supplemented with Geneticin®. The medium with antibiotics was replaced every 2–3 days until colonies of cells could be picked up and screened by immunostaining (data not shown). The selected colonies were amplified and lysed, and the lysates were studied using Western blotting. As shown in Figure 2B, the stable expression results were similar to the results shown in Figure 2A. EGFR-GGS is not phosphorylated at Tyr 1068, when assayed using anti-P-Tyr1068 antibodies. None of the other tyrosines could be phosphorylated either, as demonstrated by 4G10 staining. Thus, EGFR JM domain is critical for the phosphorylation of all tyrosines.

**The substitution of the JM domain does not affect EGFR cross-linking.** In the literature, dimerization propensities of different receptors are usually compared using chemical cross-linking<sup>18–21</sup>. We therefore compared the cross-linking propensities of EGFR and EGFR-GGS in CHO cells by incubating the cells with a membrane-impermeable linker (BS3, Pierce) prior to lysis, as described in Materials and Methods, followed by Western blotting. As shown in Figure 3A, both dimers and monomers were observed on the Western blots. In the absence of ligands, both EGFR and

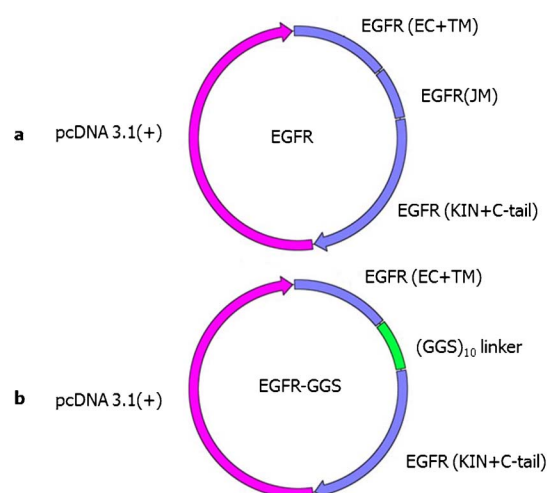


**Figure 1 | Schematics of the plasmids used in the study, encoding wild-type EGFR and EGFR-GGS.** To create the EGFR-GGS plasmid, the oligonucleotides encoding EGFR JM domain (EGFR amino acids 650–680) were removed by digestion, and annealed oligonucleotides encoding ten GGS repeats were inserted in their place as described in Materials and Methods.

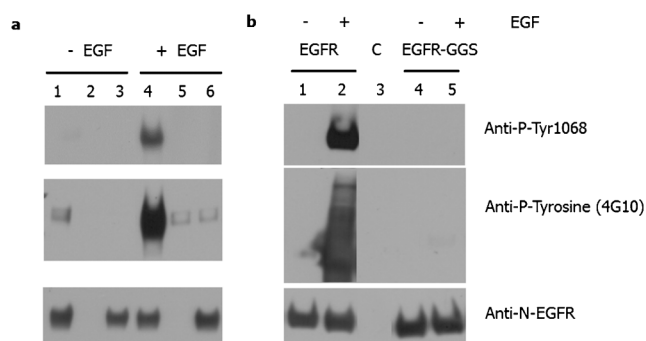


**Figure 2 | Activation of EGFR and EGFR-GGS.** (A). CHO cells were transfected with plasmids encoding EGFR (lanes 1 and 4) or EGFR-GGS (lanes 3 and 6). Lanes 2 and 5 were non-transfected CHO cells. 24 hours after transfection, cells were starved for another day, and then treated with EGF (lanes 4, 5, and 6), followed by lysis. Cell lysates were subjected to Western blotting. (B). HEK 293 cells stably expressing EGFR (lanes 1 and 2), pcDNA 3.1(+) (lane 3) and EGFR-GGS (lanes 4 and 5) were deprived of serum overnight. The cells were treated with 0 (lanes 1, 3, and 4) and 2500 ng/ml EGF (lanes 2 and 5) for 10 minutes before lysis.

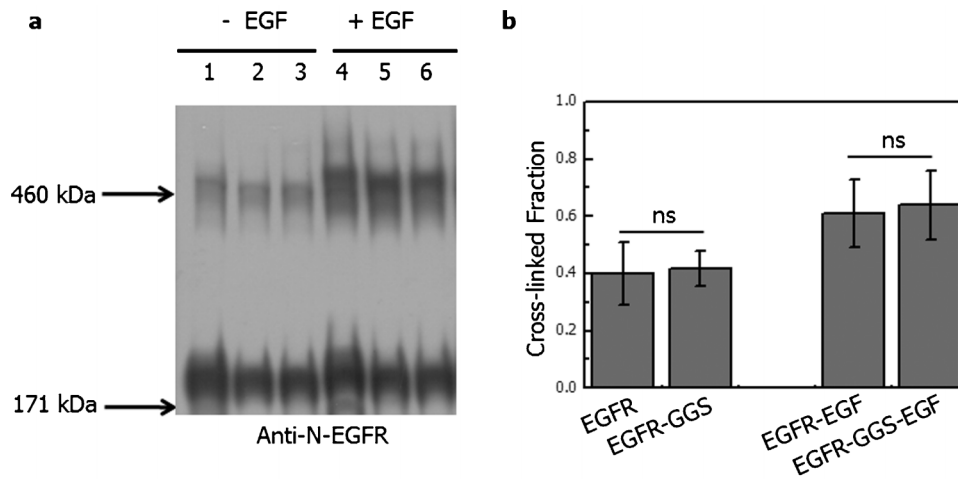


**Figure 3 | Cross-linking of EGFR and EGFR-GGS.** (A) CHO cells were transfected with plasmids encoding EGFR (lanes 1 and 4) and EGFR-GGS (lanes 2, 3, 5, and 6). 24 hours later, the normal medium was replaced by serum-free medium. After another 24 hours, cells (lanes 4, 5 and 6) were treated with 2500 ng/ml EGF for 10 minutes. Then 2 mM cross-linker BS3 was added to the cells before they were subjected to lysis. Four sets of experiments were performed, and the results are shown in (B).

EGFR-GGS exhibited dimeric bands (lanes 1 and 3), the intensities of which increased significantly after the addition of the ligand EGF (lanes 4 and 6). The cross-linked fraction was calculated as  $S_D/S = S_D/(S_M + S_D)$ , where  $S_D$  is the intensity of the dimeric band, and  $S_M$  is the intensity of the monomeric band. In the absence of ligand, cross-linked fractions varied between 0.25 to 0.5. In the presence of ligand, they varied between 0.45 to 0.9. Figure 3B shows the averages from three independent crosslinking experiments ( $0.40 \pm 0.11$  and  $0.42 \pm 0.06$  in the absence of ligand and  $0.61 \pm 0.12$  and  $0.64 \pm 0.12$  in the presence of ligand). There is no statistical significant difference between the cross-linked fractions of EGFR and EGFR-GGS ( $p = 0.57$  and  $p = 0.44$  in the absence and presence of ligand, respectively). This result indicates that EGFR cross-linking is not affected by the replacement of the JM domain with a GGS linker.

**The substitution of the JM domain does not affect the FRET efficiency as a measure of EGFR dimerization in the absence of ligand.** Recently we developed a method that allows us to directly measure membrane protein dimerization propensities in biological membranes<sup>22,23</sup>. Measurements are carried out in plasma membrane derived vesicles, which bud off cells upon treatments that perturb the actin cytoskeleton<sup>24–26</sup>. The detection of dimers is based on FRET and it thus requires the modification of the receptors with fluorescent

proteins. To pursue this line of inquiry, we created four plasmids encoding EGFR-YFP, EGFR-mCherry, EGFR-GGS-YFP, and EGFR-GGS-mCherry, respectively. Details pertaining to plasmid design and production are given in Materials and Methods.

CHO cells were cotransfected with either EGFR-YFP and EGFR-mCherry, or EGFR-GGS-YFP and EGFR-GGS-mCherry. The cells were then subjected to vesiculation as previously described, and each plasma membrane-derived vesicle was imaged in a Nikon confocal microscope<sup>22,23,27</sup>. About 80 images of vesicles were acquired for each receptor. However, the expression of these constructs in the plasma membrane was very low. Thus, as many as 80% of the vesicles could not be analyzed by the image recognition software because they were of very low intensity. The highest expression for EGFR and EGFR-GGS was an order of magnitude lower than the expression of other membrane proteins that we have studied with this methodology<sup>22,23</sup>.

In Figure 4A the measured FRET efficiencies are plotted as a function of acceptor concentration in the vesicles. Each data point in Figure 4A corresponds to a single vesicle. Data appear quite scattered, as it can be expected due to the very low receptor concentration; this scattering is due to white noise associated with image acquisition<sup>22</sup>. The solid line corresponds to FRET that is expected to occur if there are no specific interactions. We see that the

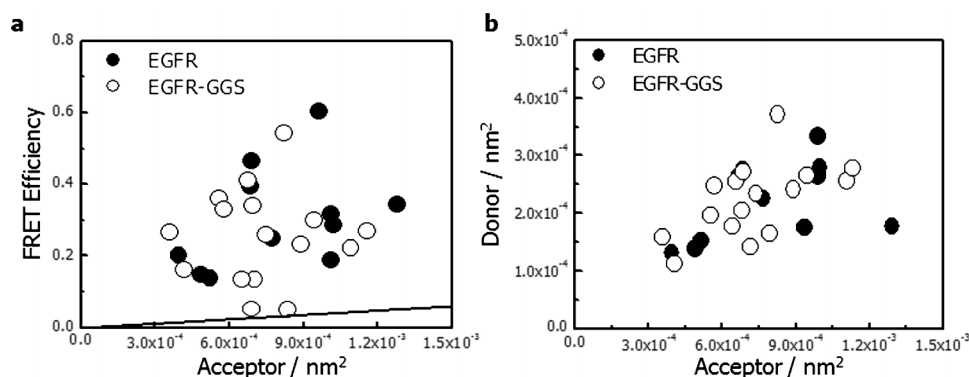


**Figure 4 | (A)** FRET efficiencies measured for EGFR (filled circles) and EGFR-GGS (open circles) in CHO plasma membrane-derived vesicles. Each data point represents a single vesicle, for which the FRET efficiency and the acceptor concentrations are determined using the QI-FRET method. Also shown is the FRET efficiency that one expects to see if the receptors do not dimerize (solid line). The measured FRET efficiency is higher than this level for both receptors. **(B)** Concentrations of the YFP (donor) and mCherry (acceptor)-tagged receptors in the vesicles analyzed in Figures A.

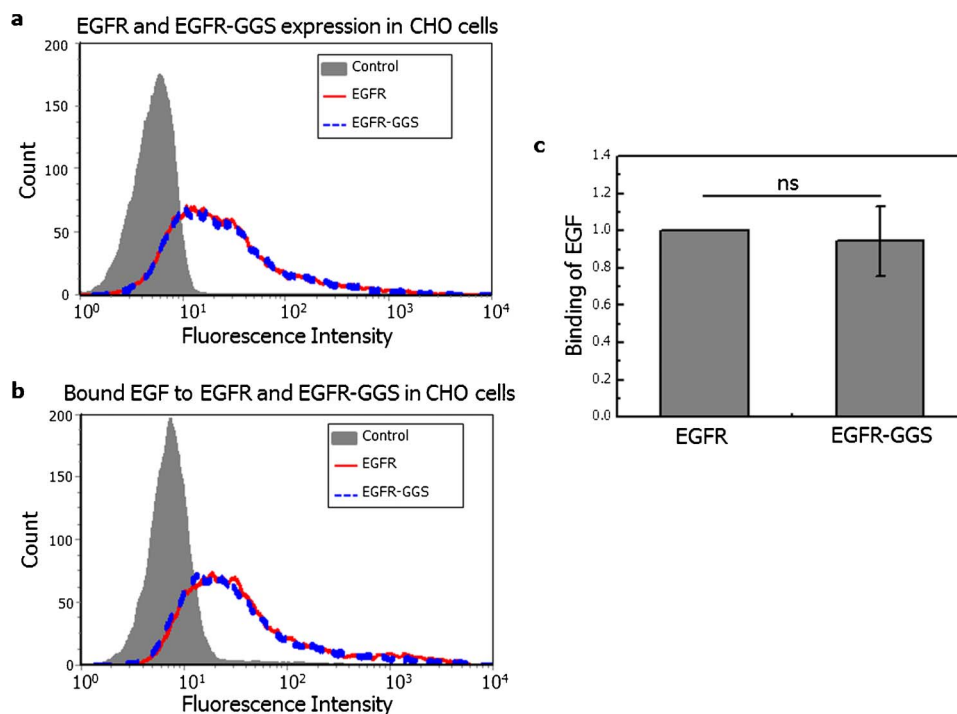


**Figure 5 | Binding of EGF to EGFR and EGFR-GGS, expressed transiently in CHO cells.** CHO cells were transfected with plasmids encoding EGFR, EGFR-GGS and pcDNA 3.1+ (control). 24 hours later, the normal medium was replaced by serum-free medium. After another 24 hours, cells were stained by Alexa Fluor-488 conjugated anti-EGFR antibodies (3A) and Alexa Fluor-488 conjugated EGF (2500 ng/ml) (3B). To quantify the binding of the receptors to EGF, the geometric means of the fluorescence intensities were calculated using the FCS software. The binding strengths of the ligand to the two receptors were calculated by dividing the binding intensities by the expression intensities, as shown in 3C. Three independent sets of experiments were performed.

measured FRET is higher than these levels, suggesting that specific interactions occur for both EGFR and EGFR-GGS.

Since the expression did not vary more than by a factor of three for all acquired data points, we averaged all the data and compared the measured FRET efficiencies for EGFR and EGFR-GGS using Student t-test. The averages  $\pm$  standard errors are  $0.29 \pm 0.05$  and  $0.25 \pm 0.04$ . The difference between the FRET efficiencies for the two receptors is not statistically significant ( $p = 0.57$ , based on Student t-test analysis). Furthermore, there are no significant differences between the expressions of the two constructs, as shown in Figure 4B.

#### Binding of EGF to EGFR is not affected by the JM domain replacement.

Next we investigated if the replacement of the JM domain affects the binding of the ligand EGF to EGFR using flow cytometry. In the first series of ligand-binding experiments, the EGF concentration was fixed at 2500 ng/ml. CHO cells were transfected with plasmids encoding EGFR/WT and EGFR-GGS, as well as an empty pcDNA 3.1 vector as control. 24 hours after transfection, the cells were starved for another day, and treated with EDTA to detach them from the substrate. The suspended cells were split into two cell pools. The first cell pool was incubated with Alexa Fluor 488-labeled anti-N-EGFR antibodies, in order to quantify the expression of the receptors. As this antibody recognized the extracellular domain of EGFR, it is reactive to both wild-type EGFR and to EGFR-GGS. The second cell pool was incubated with 2500 ng/ml Alexa Fluor 488-labeled EGF, to quantify the amount of bound EGF. After incubation on ice for half an hour and three washes, each cell pool was analyzed via flow cytometry as described in Materials and Methods. The expression of the two receptors (as reported by the fluorescence intensity of the anti-N-EGFR antibodies) and the amount of bound EGF (as reported by the fluorescence intensity of the bound EGF) are shown Figure 5A and 5B, respectively. The fluorescence histogram means were calculated using the FCS Express software (De

Novo Software), and corrected for background. To quantify ligand binding, the average bound EGF fluorescence values were divided by the respective average anti-EGFR fluorescence values. The results, shown in Figure 5C, demonstrate that there is no difference between EGF-EGFR and EGF-EGFR-GGS binding ( $p = 0.58$ ).

To validate these findings, and to explore a wider range of ligand concentrations, in the second series of ligand-binding experiments we worked with stable HEK 293 cells. In particular, we used two HEK 293 cell lines that express EGFR and EGFR-GGS at very similar levels (Figure 6A). Control HEK 293 cells, transfected with empty pcDNA 3.1 vectors, were also incubated with antibodies and ligand and analyzed at each ligand concentration. The ligand concentrations used ranged from 10 to 2500 ng/ml, as binding in this ligand concentration range was measurable in the FACS experiments. As shown in Figure 6B and 6C, the EGF staining intensities of cells expressing EGFR and EGFR-GGS increase as the concentration of ligand increases, indicative of increased binding. The quantitative results are shown in Figure 6D. To compare the binding of EGF to EGFR and to EGFR-GGS, we divided the amount of EGFR-GGS-bound ligand by the amount of EGFR-bound ligand. As shown in Figure 6E, the ratio is 1 for all tested ligand concentrations ( $p > 0.05$ ). These experiments demonstrate that the binding of EGF to EGFR is not affected by the replacement of JM domain by a (GGS)<sub>10</sub> linker, over the studied range of ligand concentrations.

#### Discussion

The intracellular JM domains of several RTKs have been shown to play autoinhibitory roles by blocking the substrate entry into the nucleotide-binding pocket<sup>28–32</sup>. EGFR JM domain, on the other hand, has been suggested to play a distinctly different, activating role. Thiel et al. deleted the whole JM domain from the ErbB1 intracellular domain and observed a severe loss of intracellular domain tyrosine



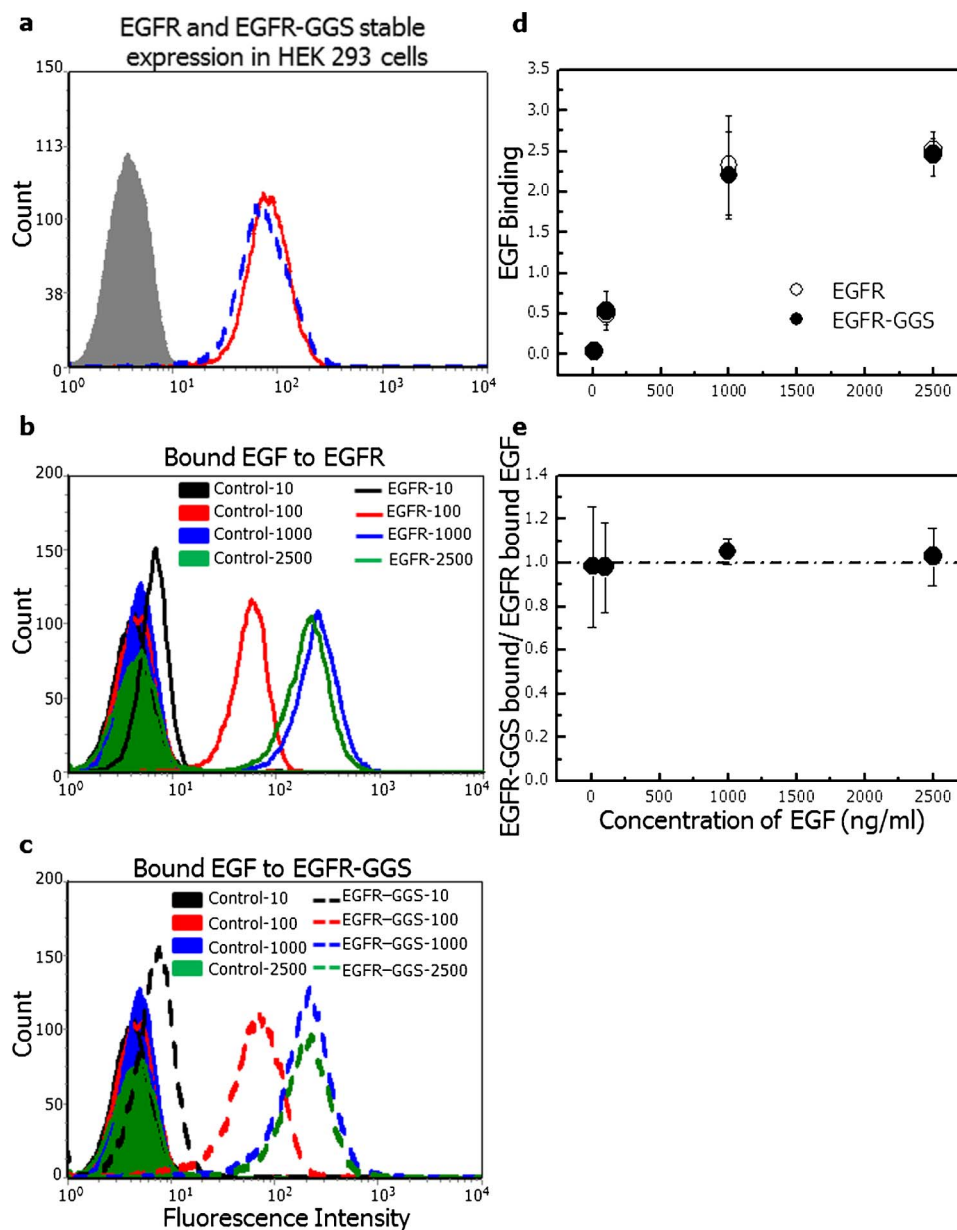


**Figure 6** | Binding of EGF to EGFR and EGFR-GGS, expressed stably in HEK cells. (A) Flow cytometry data for HEK 293 cells stably expressing EGFR, EGFR-GGS and empty pcDNA 3.1 (+) vectors. Cells were stained with Alexa Fluor-488 conjugated anti-EGFR antibodies or Alexa Fluor-488 conjugated EGF at concentrations of 10, 100, 1000 and 2500 ng/ml. (B) Binding of EGF, at different concentrations, to EGFR. (C) Binding of EGF, at different concentrations, to EGFR-GGS. (D) The geometric means of the fluorescence intensities of bound antibodies and bound ligands were calculated using the FCS software. EGF binding was normalized by the receptor expression levels. (E) Ratios of EGFR-bound EGF to EGFR-GGS bound EGF, as a function of EGF concentrations.

phosphorylation<sup>16</sup>. Brewer et al. used alanine scanning mutagenesis and demonstrated that mutations in the C-terminal 19 residues of the EGFR JM region (664–682) abolished EGFR activation<sup>33</sup>. In this work, we designed a chimeric receptor in which the JM domain of EGFR is replaced by a 30-amino acid long (GGS)<sub>10</sub> linker, such that the chimeric receptor is very similar and of the same length as wild type EGFR. This substitution is not expected to affect the TM and kinase domains because GGS-linkers have been shown to decouple the proteins that they are linked to, and not to perturb their structure and function<sup>17</sup>. This construct allowed us to study the effect of the JM domain on EGFR activation without introducing structural constraints within the EGFR dimers. After the replacement, we observed a complete abolishment of EGFR phosphorylation at all tyrosine sites (Figure 2). This result is consistent with published results and

highlights the critical role that EGFR JM domain plays in EGFR activation.

Here we also investigated the role of the JM domain in ligand-independent EGFR dimerization. We performed both cross-linking and FRET experiments in the absence of ligand. We observed cross-linked bands in the Western blots for both EGFR and EGFR-GGS. We also observed high FRET efficiencies for the two receptors. These results suggest that both receptors form dimers in the absence of ligand. As shown in Figure 3B, about 40% of the receptors are cross-linked. Yet, we see no EGFR-GGS activity in all cases, no EGFR activity in the stable cell lines, and very weak EGFR activity in the transient transfection experiments. Thus, all EGFR-GGS and the majority of EGFR molecules are inactive in the absence of ligand.



While details about the inactive dimer are unknown, Jura et al crystallized a symmetric kinase dimer, presumably in the inactive conformation<sup>14</sup>. Contacts between the two kinase domains in this inactive dimer are mediated by parts of the C-terminal tail. In particular, residues 967 to 978 form a helix which packs against the neighboring kinase, while residues 979–981 salt-bridge with residues on the neighboring kinase. Additional insight about the structure of the EGFR unliganded dimer comes from experiments performed by Linda Pike and colleagues, who used luciferase complementation imaging to follow conformational changes in the receptor upon ligand stimulation<sup>34</sup>. The two fragments of the luciferase complementation system, NLuc and CLuc were fused to the C-terminus of EGFR. These fragments are not capable of producing light by themselves as monomers but are capable of forming an active luciferase if brought into close proximity. The researchers observed significant luciferase activity in the absence of ligand, which suggested that the unliganded EGFR dimer adopted a conformation in which the C-terminal tails of the two monomers were in close proximity of each other, such that the two fragments can form a functional enzyme<sup>34</sup>. This is generally consistent with Jura's crystal structure of the inactive dimer<sup>14</sup>. Since the C-terminal tail packs at the interface between the two kinases, it is likely that the two terminal ends to which NLuc and CLuc are attached are also in close proximity such that a functional luciferase can be formed<sup>34</sup>.

The attachment of the fluorescent proteins in our FRET experiments was the same as in Pike's experiments, and therefore the fluorescent proteins in the dimer are expected to be in close proximity of each other. The dimeric fractions ( $f$ ) can be obtained from the FRET efficiencies using the following equation<sup>35</sup>:

$$f = \frac{E_D}{X_A \tilde{E}} \quad (1)$$

In this equation  $E_D$  is the measured FRET efficiency (symbols in Figure 4A), corrected for the FRET due to random proximity of donors and acceptors (solid line in Figure 4A).  $X_A$  is the acceptor fraction (concentration of acceptors over concentration of donors and acceptors), which is known, i.e. determined with the QI-FRET method. The parameter  $\tilde{E}$  is the FRET efficiency of a dimer with both a donor and an acceptor present. The value of  $\tilde{E}$  is dependent upon the separation distance between the donor and the acceptor in the dimer, i.e. on the structure of the dimer. As the experiments of Pike and colleagues suggest that the fluorescent proteins are in close proximity, we can estimate the distance between them and therefore we can estimate  $\tilde{E}$ <sup>34</sup>. As the size of the fluorescent proteins is about 40 Å, the closest possible distance between the two fluorophores is 40 Å. Since the Förster radius is 53 Å,  $\tilde{E}$  can be calculated as 84%, and the dimeric fraction for EGFR should be about 40%. Even if we assume that the distance between the two fluorophores is 50 Å, the dimeric fraction of EGFR would be about 55%. These back-of-the-envelope calculations suggest that about 40 to 50% of the receptors pre-dimerize in the absence of ligand, consistent with the cross-linking results in Figure 3. As the FRET efficiencies recorded for EGFR and EGFR-GGS are the same (Figure 4), and the crosslinked fractions are the same (Figure 3), it is likely that  $\tilde{E}$  is the same for both receptors. We can thus speculate that the structures of the kinase dimers in the unliganded EGFR and EGFR-GGS dimers are the same, and likely the same as the symmetric inactive structure proposed by Jura and colleagues<sup>14</sup>. As we do not expect any stabilizing contacts between the (GGG)<sub>10</sub> unstructured sequences in EGFR-GGS, we deduce that there are no direct JM-JM domain stabilizing contacts in the inactive EGFR dimer.

Next we asked whether the abolished phosphorylation at high ligand concentration is at least in part due to aberrations in ligand binding. This was a possibility, since experiments by Macdonald-Obermann and Pike have suggested that the JM domain affects

ligand binding to EGFR via an intricate allosteric mechanism<sup>15</sup>. To investigate if binding is affected by the substitution of EGFR JM domain with the (GGG)<sub>10</sub> flexible linker, we first assayed ligand binding in transient transfection experiments at high ligand concentration. We saw no differences in the ligand binding affinities of EGFR and EGFR-GGS (Figure 5). This result suggests that the loss of intracellular tyrosine kinase activity at saturating ligand concentration that we observe after the replacement of the JM domain with the (GGG)<sub>10</sub> linker does not occur because of impaired ligand binding.

To further our confidence in this conclusion, we created HEK 293 stable lines that exhibit the same EGFR and EGFR-GGS expression, and we studied ligand binding over the ligand concentration range from 10 ng/ml to 2500 ng/ml. Again, we saw no differences in the ligand binding affinities of EGFR and EGFR-GGS (Figures 6) over the ligand concentration range that was accessible in the FACS experiments.

The results presented here can give insight into the role of the JM domain in EGFR activation models. There are models of EGFR activation in the literature which describe some experimental data very well, such as the “model of EGF binding in an aggregating system” proposed by Linda Pike and colleagues<sup>36</sup>. In this model EGFR monomers and dimers coexist in the absence of ligand, and ligand can bind to monomers, to unoccupied dimers, or to dimers bound to one ligand. However, the activation of EGFR is a very complex process, and even this model is likely an oversimplification, since it does not account explicitly for EGFR activation in the liganded state, i.e. for the transition from an inactive to an active dimer upon ligand binding.

In our experiments we see a substantial population of inactive dimers in the absence of ligand, consistent with previous reports<sup>37–40</sup>. Therefore, we can assume that a large fraction of EGFR molecules likely gets activated in a three-step process consisting of: (1) EGFR dimerization in the absence of ligand, yielding an inactive dimer, (2) ligand binding to this dimer, followed by a (3) transition to an active dimer. It is already known that the final active state cannot be attained without the JM domain. Here we demonstrate that the JM domain does not stabilize the inactive EGFR dimer. We also demonstrate that JM domain does not affect ligand binding at high ligand concentration. Our results therefore suggest that the major role of the JM domain is in the last step of EGFR activation, the transition from the inactive to an active dimer.

## Methods

**Plasmid constructs.** The pcDNA3.1-EGFR plasmid was a generous gift from Professor Daniel Leahy, Johns Hopkins University. To replace the 30 amino acid-long JM domain by 10 GGS repeats, we created two restriction enzyme sites in the pcDNA3.1-EGFR plasmid using a multisite mutagenesis kit (Stratagene). In particular, a HindIII site was introduced before the JM domain and an EcoRI site was introduced after the JM domain. The plasmid was then double digested. DNA oligomers encoding ten GGS repeats were synthesized by Invitrogen and ligated to the digested pcDNA3.1-EGFR vector to create pcDNA3.1-EGFR-GGS. The successful substitution of EGFR JM domain with a (GGG)<sub>10</sub> linker was confirmed by sequencing provided by Genewiz (Germantown, MD). To tag the receptors with fluorescent proteins at the C-terminus, the genes encoding EGFR and EGFR-GGS were amplified using PCR and the stop codons were removed. The PCR products were ligated between the NheI and KpnI sites in the pcDNA 3.1 (+) vector. The genes encoding the fluorescent proteins were amplified by PCR and two restriction enzyme sites were created: a KpnI site before the fluorescent protein DNA, and an XbaI site was after the stop codon. The amplified genes were inserted between the KpnI and the XbaI sites in pcDNA 3.1-EGFR and pcDNA 3.1-EGFR-GGS.

**Cell culture.** CHO cells were cultured in Dulbecco's modified Eagle's medium (Invitrogen, CA) supplemented with 10% fetal bovine serum (Thermo Scientific) and nonessential amino acids (Gibco, CA). Human embryonic kidney (HEK) 293 cells were cultured in DMEM supplemented with 10% fetal bovine serum (FBS). All cells were maintained in the incubator with 5% CO<sub>2</sub> at 37°C.

**Creation of stable cell lines.** HEK 293 cells were transfected with pcDNA3.1-EGFR-GGS, pcDNA3.1-EGFR, or pcDNA 3.1(+) empty vectors using Fugene HD (Roche Applied Science) following the manufacturer's protocol. Twenty four hours after



transfection, the culture medium was replaced by medium supplemented with 0.6  $\mu\text{g}/\text{ml}$  Geneticin<sup>®</sup> (G418, Invitrogen). Two or 3 days later, the cells that grew to about 90% confluency were passed and seeded with high dilution ratio into 150-mm cell culture dishes. The medium with antibiotics was replaced every 2–3 days until colonies of cells appeared around 2 weeks after the initial seeding. 12 colonies from each dish were selected and cultured in 24-well plates. The expression levels of EGFR and EGFR-GGS were estimated by immunostaining, and further assayed by Western blots and Flow Cytometry.

**Western blots.** CHO cells were transfected with either pcDNA3.1-EGFR-GGS or pcDNA3.1-EGFR, or pcDNA 3.1(+) empty vectors. These cells, as well as the HEK 293 stable cell lines, were starved in serum-free DMEM for 24 hours. The cells were treated with lysis buffer [25 mM Tris-HCl, 0.5% Triton X-100, 20 mM NaCl, 2 mM ethylenediaminetetraacetic acid, 2 mM NaVO<sub>4</sub> and protease inhibitor (Roche Applied Science)]. After centrifugation at 15,000 *g* for 15 min at 4°C, the supernatant was collected, and the pellet was discarded. Protein concentration was determined using the BCA™ assay kit (Pierce, IL). The lysates were loaded into 3–8% NuPAGE<sup>®</sup> Novex<sup>®</sup> Tris-acetate mini gels (Invitrogen). Proteins were separated by electrophoresis and transferred onto a nitrocellulose membrane. The membrane was blocked with milk for 1 h at room temperature and then stained with anti-N-EGFR antibodies (Cell Signaling Technology), anti-P-Tyr1068 antibodies (Cell Signaling Technology), anti-phospho-Tyr, clone 4G10<sup>®</sup> antibodies (Millipore). The secondary antibodies were either anti-rabbit or anti-mouse horseradish-peroxidase-conjugated antibodies (Promega, WI). ECL™ detection reagent (GE Healthcare Life Sciences, UK) was used to visualize the Western blot bands. The bands were quantified using ImageQuant TL (GE Healthcare Life Sciences).

The Western blot films were scanned and processed with ImageQuant TL. At least three sets of independent experiments were performed to determine the averages and the standard deviations as described<sup>41–45</sup>.

**Flow cytometry measurements.** Cells were starved in serum-free DMEM for 24 hours and then incubated in 5 mM EDTA and washed with 3% FBS/PBS. EGFR and EGFR-GGS expressed on the cell surface were detected with anti-N-EGFR antibodies conjugated with Alexa Fluoro 488 (Santa Cruz biotechnology). The binding of EGF to the receptors was measured using Alexa Fluoro 488 conjugated EGF (Invitrogen). Measurements were performed with a FACSCalibur flow cytometer (BD Biosciences). The expression levels of EGFR and EGFR-GGS, and the binding of EGF to the receptors was determined using the FCS express software (De Novo Software).

**Cross-linking.** In cross-linking experiments, dimeric EGFR or EGFR-GGS receptors were cross-linked with a membrane-impermeable cross-linker BS3 (bis(sulfosuccinimidyl) suberate, Pierce). Twenty four hours after transfection, cells were incubated with 2 mM cross-linker for 30 min at room temperature and then quenched in 20 mM Tris-HCl for 15 min. After a rinse with ice-cold PBS, the cells were lysed, and the receptors were detected using Western blotting. The cross-linked fraction was calculated as  $S_D/S = S_D/(S_M + S_D)$ , where  $S_D$  is the intensity of the dimeric band, and  $S_M$  is the intensity of the monomeric band.

**Vesiculation.** CHO cells were seeded in a 6-well plate at a density of  $6 \times 10^4$  cells/well one day prior to transfection. Cells were transfected using Eugene HD (Roche Applied Science) following the manufacturer's protocol. Cells were co-transfected with pcDNA\_EGFR\_YFP and pcDNA\_EGFR\_mCherry or pcDNA\_EGFR-GGS-YFP and pcDNA\_EGFR-GGS-mCherry. Vesiculation was performed using a previously described method<sup>24–26</sup>. Briefly, cells were rinsed twice with PBS (pH 7.4) containing 0.75 mM calcium and 0.5 mM magnesium (CM-PBS), and once with vesiculation buffer consisting of CM-PBS with 25 mM formaldehyde and 0.5 mM 1,4-dithiothreitol (DTT). The cells were then incubated at 37°C with 1 mL of vesiculation buffer for 2 hours. To quench the formaldehyde in the vesiculation buffer, glycine solution was added to a final concentration of 0.125 M. These vesicles have been shown to be an adequate model of the plasma membrane<sup>46</sup>. The vesicles were transferred into an 8-well Nunc Lab-Tek II chamber slide and allowed to settle for 1 hour before imaging.

**FRET experiments.** Images of vesicles were acquired using a Nikon Eclipse confocal laser scanning microscope with a 60X water immersion objective. All the images were collected and stored at a 512×512 resolution. Three different scans were performed for each vesicle: (1) excitation at 488 nm, with a 500–530 nm emission filter (donor scan); (2) excitation at 488 nm, with a 565–615 nm emission filter (FRET scan); and (3) excitation at 543 nm, with a 650 nm long-pass filter (acceptor scan). Gains of 8.0 were used for all the three scans. To minimize the bleaching of fluorescent proteins, ND8 filters were used during excitation with the 488 nm laser, and pixel dwell time was set to the minimum (1.68  $\mu\text{s}$ ). These images were analyzed with a Matlab program developed in the lab, which automatically recognizes the vesicles and calculates the intensities in the three channels as previously described<sup>22,23</sup>.

**Statistical analysis.** All experiments were repeated at least three times to determine the averages and the standard deviations. Student t-test was used to compare the measurements to a null hypothesis for statistical significance, as previously described<sup>43,44</sup>. The p-value cutoff for significance is 0.05.

1. Wells, A. EGF receptor. *International Journal of Biochemistry & Cell Biology* **31**, 637–643 (1999).

2. Linggi, B. & Carpenter, G. ErbB receptors: new insights on mechanisms and biology. *Trends in Cell Biology* **16**, 649–656 (2006).
3. Grandis, J. R. & Sok, J. C. Signaling through the epidermal growth factor receptor during the development of malignancy. *Pharmacology & Therapeutics* **102**, 37–46 (2004).
4. Drevs, J., Medinger, M., Schmidt-Gerbach, C., Weber, R. & Unger, C. Receptor Tyrosine Kinases: The Main Targets for New Anticancer Therapy. *Current Drug Targets* **4**, 113–121 (2003).
5. Pantaleo, M. A. *et al.* Molecular imaging and targeted therapies in oncology: New concepts in treatment response assessment. A collection of cases. *International Journal of Oncology* **33**, 443–452 (2008).
6. Schlessinger, J. Cell signaling by receptor tyrosine kinases. *Cell* **103**, 211–225 (2000).
7. Eswarakumar, V. P., Lax, I. & Schlessinger, J. Cellular signaling by fibroblast growth factor receptors. *Cytokine Growth Factor Rev.* **16**, 139–149 (2005).
8. Schlessinger, J. Common and distinct elements in cellular signaling via EGF and FGF receptors. *Science* **306**, 1506–1507 (2004).
9. Zhang, X. W., Gureasko, J., Shen, K., Cole, P. A. & Kuriyan, J. An allosteric mechanism for activation of the kinase domain of epidermal growth factor receptor. *Cell* **125**, 1137–1149 (2006).
10. Burgess, A. W. *et al.* An open-and-shut case? Recent insights into the activation of EGF/ErbB receptors. *Molecular Cell* **12**, 541–552 (2003).
11. Alvarado, D., Klein, D. E. & Lemmon, M. A. Structural Basis for Negative Cooperativity in Growth Factor Binding to an EGF Receptor. *Cell* **142**, 568–579 (2010).
12. Escher, C., Cymer, F. & Schneider, D. Two GxxxG-Like Motifs Facilitate Promiscuous Interactions of the Human ErbB Transmembrane Domains. *J. Mol. Biol.* **389**, 10–16 (2009).
13. Chen, L., Merzlyakov, M., Cohen, T., Shai, Y. & Hristova, K. Energetics of ErbB1 transmembrane domain dimerization in lipid bilayers. *Biophys. J.* **96**, 4622–4630 (2009).
14. Jura, N. *et al.* Mechanism for Activation of the EGF Receptor Catalytic Domain by the Juxtamembrane Segment. *Cell* **137**, 1293–1307 (2009).
15. Macdonald-Obermann, J. L. & Pike, L. J. The Intracellular Juxtamembrane Domain of the Epidermal Growth Factor (EGF) Receptor Is Responsible for the Allosteric Regulation of EGF Binding. *J. Biol. Chem.* **284**, 13570–13576 (2009).
16. Thiel, K. W. & Carpenter, G. Epidermal growth factor receptor juxtamembrane region regulates allosteric tyrosine kinase activation. *Proceedings of the National Academy of Sciences of the United States of America* **104**, 19238–19243 (2007).
17. Evers, T. H., van Dongen, E. M. W. M., Faesen, A. C., Meijer, E. W. & Merx, M. Quantitative understanding of the energy transfer between fluorescent proteins connected via flexible peptide linkers. *Biochemistry* **45**, 13183–13192 (2006).
18. Fanger, B. O., Stephens, J. E. & Staros, J. V. High-Yield Trapping of EGF-Induced Receptor Dimers by Chemical Cross-Linking. *FASEB J.* **3**, 71–75 (1989).
19. Monsonego-Ornan, E., Adar, R., Feferman, T., Segev, O. & Yayon, A. The transmembrane mutation G380R in fibroblast growth factor receptor 3 uncouples ligand-mediated receptor activation from down-regulation. *Mol. Cell. Biol.* **20**, 516–522 (2000).
20. Weiner, D. B., Liu, J., Cohen, J. A., Williams, W. V. & Greene, M. I. A Point Mutation in the Neu Oncogene Mimics Ligand Induction of Receptor Aggregation. *Nature* **339**, 230–231 (1989).
21. Angers, S. *et al.* Detection of beta(2)-adrenergic receptor dimerization in living cells using bioluminescence resonance energy transfer (BRET). *Proceedings of the National Academy of Sciences of the United States of America* **97**, 3684–3689 (2000).
22. Chen, L., Novicky, L., Merzlyakov, M., Hristov, T. & Hristova, K. Measuring the Energetics of Membrane Protein Dimerization in Mammalian Membranes. *J. Am. Chem. Soc.* **132**, 3628–3635 (2010).
23. Chen, L., Placone, J., Novicky, L. & Hristova, K. The extracellular domain of fibroblast growth factor receptor 3 inhibits ligand-independent dimerization. *Science Signaling* **3**, ra86 (2010).
24. Scott, R. E. Plasma membrane vesiculation: A new technique for isolation of plasma membrane. *Science* **194**, 743–745 (1976).
25. Scott, R. E. & Maercklein, P. B. Plasma-Membrane Vesiculation in 3T3-Cells and Sv3T3 Cells .2. Factors Affecting the Process of Vesiculation. *J. Cell Sci.* **35**, 245–252 (1979).
26. Scott, R. E., Perkins, R. G., Zschunke, M. A., Hoerl, B. J. & Maercklein, P. B. Plasma-Membrane Vesiculation in 3T3-Cells and Sv3T3-Cells .1. Morphological and Biochemical Characterization. *J. Cell Sci.* **35**, 229–243 (1979).
27. Li, E., Placone, J., Merzlyakov, M. & Hristova, K. Quantitative measurements of protein interactions in a crowded cellular environment. *Anal. Chem.* **80**, 5976–5985 (2008).
28. Chang, P. M., Ilangumaran, S., La Rose, J., Chakrabarty, A. & Rottapel, R. Autoinhibition of the Kit receptor tyrosine kinase by the cytosolic juxtamembrane region. *Mol. Cell. Biol.* **23**, 3067–3078 (2003).
29. Griffith, J. *et al.* The structural basis for autoinhibition of FLT3 by the juxtamembrane domain. *Molecular Cell* **13**, 169–178 (2004).
30. Binns, K. L., Taylor, P. P., Sicheri, F., Pawson, T. & Holland, S. J. Phosphorylation of tyrosine residues in the kinase domain and juxtamembrane region regulates the biological and catalytic activities of eph receptors. *Mol. Cell. Biol.* **20**, 4791–4805 (2000).



31. Mol, C. D. *et al.* Structure of a c-Kit product complex reveals the basis for kinase transactivation. *J. Biol. Chem.* **278**, 31461–31464 (2003).
32. Wybenga-Groot, L. E. *et al.* Structural basis for autoinhibition of the EphB2 receptor tyrosine kinase by the unphosphorylated juxtamembrane region. *Cell* **106**, 745–757 (2001).
33. Brewer, M. R. *et al.* The Juxtamembrane Region of the EGF Receptor Functions as an Activation Domain. *Molecular Cell* **34**, 641–651 (2009).
34. Yang, K. S., Ilagan, M. X. G., Piwnica-Worms, D. & Pike, L. J. Luciferase Fragment Complementation Imaging of Conformational Changes in the Epidermal Growth Factor Receptor. *J. Biol. Chem.* **284**, 7474–7482 (2009).
35. Merzlyakov, M. & Hristova, K. Forster Resonance Energy Transfer Measurements of Transmembrane Helix Dimerization Energetics. *Methods in Enzymology: Fluorescence Spectroscopy* **450**, 107–127 (2008).
36. Macdonald, J. L. & Pike, L. J. Heterogeneity in EGF-binding affinities arises from negative cooperativity in an aggregating system. *Proceedings of the National Academy of Sciences of the United States of America* **105**, 112–117 (2008).
37. Kozer, N. *et al.* Evidence for extended YFP-EGFR dimers in the absence of ligand on the surface of living cells. *Physical Biology* **8** (2011).
38. Chung, I. *et al.* Spatial control of EGF receptor activation by reversible dimerization on living cells. *Nature* **464**, 783–U163 (2010).
39. Yu, X. C., Sharma, K. D., Takahashi, T., Iwamoto, R. & Mekada, E. Ligand-independent dimer formation of epidermal growth factor receptor (EGFR) is a step separable from ligand-induced EGFR signaling. *Mol. Biol. Cell* **13**, 2547–2557 (2002).
40. Moriki, T., Maruyama, H. & Maruyama, I. N. Activation of preformed EGF receptor dimers by ligand-induced rotation of the transmembrane domain. *J. Mol. Biol.* **311**, 1011–1026 (2001).
41. He, L. & Hristova, K. Pathogenic activation of receptor tyrosine kinases in mammalian membranes. *J. Mol. Biol.* **384**, 1130–1142 (2008).
42. Chen, F. H. & Hristova, K. The Physical Basis of FGFR3 Response to fgf1 and fgf2. *Biochemistry* **50**, 8576–8582 (2011).
43. He, L., Wimley, W. C. & Hristova, K. FGFR3 heterodimerization in achondroplasia, the most common form of human dwarfism. *J. Biol. Chem.* **286**, 13272–13281 (2011).
44. He, L. J., Shobnam, N. & Hristova, K. Specific inhibition of a pathogenic receptor tyrosine kinase by its transmembrane domain. *Biochimica et Biophysica Acta-Biomembranes* **1808**, 253–259 (2011).
45. He, L. J., Hoffmann, A. R., Serrano, C., Hristova, K. & Wimley, W. C. High-Throughput Selection of Transmembrane Sequences That Enhance Receptor Tyrosine Kinase Activation. *J. Mol. Biol.* **412**, 43–54 (2011).
46. Del Piccolo, N., Placone, J., He, L., Agudelo, S. C. & Hristova, K. Production of plasma membrane vesicles with chloride salts and their utility as a cell membrane mimetic for biophysical characterization of membrane protein interactions. *Anal. Chem.* **84**, 8650–8655 (2012).

## Acknowledgement

Supported by NIH GM68619. We thank Prof. Daniel Leahy for helpful discussions.

## Author contributions

LH performed the experiments and prepared the figures. LH and KH wrote and reviewed the manuscript text.

## Additional information

**Competing financial interests:** The authors declare no competing financial interests.

**License:** This work is licensed under a Creative Commons Attribution-NonCommercial-NoDerivative Works 3.0 Unported License. To view a copy of this license, visit <http://creativecommons.org/licenses/by-nc-nd/3.0/>

**How to cite this article:** He, L. & Hristova, K. Consequences of replacing EGFR juxtamembrane domain with an unstructured sequence. *Sci. Rep.* **2**, 854; DOI:10.1038/srep00854 (2012).